We are IntechOpen,
the world's leading publisher of
Open Access books
Built by scientists, for scientists

6,900
Open access books available

186,000
International authors and editors

200M
Downloads

Our authors are among the

154
Countries delivered to

TOP 1%
most cited scientists

12.2%
Contributors from top 500 universities

CLARIVATE ANALYTICS
BOOK CITATION INDEX
INDEXED

WEB OF SCIENCE™

Selection of our books indexed in the Book Citation Index
in Web of Science™ Core Collection (BKCI)

Interested in publishing with us?
Contact book.department@intechopen.com

Numbers displayed above are based on latest data collected.
For more information visit www.intechopen.com

Chemical Quantification of Mo-S, W-Si and Ti-V by Energy Dispersive X-Ray Spectroscopy

Carlos Angeles-Chavez[*],
Jose Antonio Toledo-Antonio and Maria Antonia Cortes-Jacome
Instituto Mexicano del Petróleo, Programa de Ingeniería Molecular,
Eje Central Lázaro, D.F. México
Mexico

1. Introduction

Elemental chemical identification of a specimen and its quantification is fundamental to obtain information in the characterization of the materials (Angeles et al., 2000; Cortes-Jacome et al., 2005). Energy dispersive X-ray spectroscopy (EDXS) is the technique that allows obtaining information concerning the elemental chemical composition using the EDX spectrometer. Generally is attached to a scanning electron microscope (SEM) (Goldstein & Newbury, 2003) and/or in a transmission electron microscope (Williams & Barry-Carter, 1996). The technique is very versatile because the spectrometer gives results in few minutes. The instrument is compact, stable, robust and easy to use and its results can be quickly interpreted. The analysis is based in the detection of the characteristic X-rays produced by the electron beam-specimen interaction. The information can be collected in very specific local points or on the whole sample. So, both electron microscopy and EDXS, give valuable information about the morphology and chemical composition of the sample.

In order to give an accurate interpretation of the data collected by the instrument is important to know the fundaments of the technique. The characteristic X-rays are produced by the atoms of the sample in a process called inner-shell ionization (Jenkins & De Dries, 1967). This process is carried out when an electron of inner-shell is removed by an electron of the beam generating a vacancy in the shell. At this moment the atom remain ionized during 10^{-14} second and then an electron of outer-shell fills the vacancy of the inner-shell. During this transition a photon is emitted with a characteristic energy of the chemical element and its shell ionized. The emitted photons are named by the shell-ionized type as K, L, M lines.... and α, β, γ... by the outer-shell corresponding to the electron that filled the inner-shell-ionized. For atoms with high atomic numbers, is important to note that some transitions are forbidden. Permissible transitions can be followed by the quantum selection rules and the notation can be followed by Manne Siegbahn and/or, IUPAC rules (Herglof & Birks, 1978). During the beam-sample interaction, another X-ray source is produced and it is known as Bremsstrahlung radiation or continuum X-rays which are generated for the deceleration of the electron beam in the Coulombic field of the specimen atoms. When the electrons are braked, they emit photons with any energy value giving rise to a continuous electromagnetic spectrum appearing in the EDX spectrum as

---

*Corresponding Author

background. In the case of high overvoltage, more than one electron may be ejected simultaneously from an atom and then, X-rays known as satellites peaks are generated (Deutcsh, et al., 1996). This simultaneous ejection of electrons causes a change in the overall structure of the energy levels resulting in the production of X-rays with slightly lower energies than those produced during single electron ionization appearing near to the characteristic peaks. Another important source of satellite peaks is the Auger process. Finally, in the X-ray spectrum can be detected shifts of peaks produced from a pure element and that produced by the same element contained in a compound. This variation occurs because the electronic configuration of the inner-shells of an atom is strongly influenced by the outer valence electrons. These shifts are most apparent when comparing metals with their corresponding oxides and halides. Consequently, it is not advisable to use a metallic standard material for analysis of oxide compounds. In the case of energy-dispersive X-ray analysis, the shifts of the peaks are undetectable and metals can be used as reference standards for quantification (Liebhafsky, 1976). All X-rays produced in the sample are detected and displayed in the EDX spectrum. Their identification in the spectrum is important because help to do an accurate identification of the chemical components remaining in the specimen and subsequently a more accurate quantification can be obtained. From all X-rays displayed in an EDX spectrum the most important are characteristic X-rays.

Another important parameter to consider in the EDXS is the acquisition of the data (Kenik, 2011; Scholossmacher, et al., 2010). The X-ray processing produced in the specimen is performed in three parts: detector, electronic processor and multichannel analyzer display. The overall process occurs as follow: the detector generates a charge pulse proportional to the X-ray energy. The produced pulse is first converted to a voltage and then the voltage signal is amplified through a field effect transistor, isolated from other pulses, further amplified, then identified electronically as resulting from an X-ray of specific energy. Finally, a digital signal is stored in a channel assigned to that energy in the multichannel analyzer. The speed of this process is such that the spectrum seems to be generated in parallel with the full range of X-ray energies detected simultaneously. Currently, the new software's generation delivers a spectrum ready to analyze and the previous process is not seen. However, there are many variables that must be taken into account to make a more accurate identification and subsequently their quantification. The most important variables are the time constant (Tc), acceleration voltage (AV), dead time (DT), acquisition time (AT), magnification and work distance (WD) which have direct effect on the energy resolution, peak intensity and natural width of characteristic X-ray lines. It is important to note that the calculation of the chemical composition is carried out considering the intensity and peak broadening in conjunction with the atomic number effect (Z), absorption correction (A) and characteristic fluorescence correction (F) (Newbury et al., 1986). For every group of samples with similar chemical components is recommendable to do a review of some of the previously mentioned operation variables to assure the truthfulness of the results. The chemical quantification has been very well studied for metals; however for powder samples of metallic and non-metallic oxides deposited on carbon tape, little work has been realized especially when the energy lines of two elements overlap. Generally, the chemical analysis in the scanning electron microscope can be obtained at different voltage, magnification, etc. depending on the information that it wants to reveal of a sample (Chung, et al., 1974). But if the overall chemical composition of the specimen analyzed is the primary requirement then a review of operation parameters of the instrument should be performed to ensure the accuracy of the results. In this study, the influence of operation conditions is presented to

obtain overall elemental chemical composition representative of the sample by EDXS. Specifically of elements with overlapping characteristic X-ray lines.

In order to carry out this study the Mo-S, W-Si and Ti-V systems were choice because they are widely used in the catalysis field and their accurate chemical composition are required. Additionally, their more intense characteristic X-ray lines used to calculate the composition are overlapped. In order to know if the instrument is able to solve this problematic giving reliable composition results, samples of known Mo, S, W and V composition were prepared.

2. Experimental section

Samples of Al_2O_3, MoO_3 and $S-MoO_3$, $V_2O_5-TiO_2$ and SiO_2-WO_3 were chemically analyzed in an EDX spectroscope EDAX which is attached to the environmental scanning electron microscope PHILIPS XL30. The EDAX instrument has a detector type UTW-Sapphire, an energy resolution of 0.129 keV, tilt of 0.0 and take-off of 35.90. As the microscope is designed to operate at different conditions and to obtain useful information of the samples, a review of the variables of time constant, acceleration voltage and acquisition time in order to obtain more accurate overall quantification results was performed. In this study, the dead time, the magnification and the work distance were kept constant. The DT was adjusted with the spot size and it kept around of 30%. The deconvolutions of the experimental results were followed using the Phoenix software version 3.3 included with the instrument. The software uses the so-called segment Kramer´s fit method to model the background which include the collection efficiency of the detector, the processing efficiency of the detector and the absorption of X-ray within the specimen. This method is useful when the spectrum contains overlapping peaks. The chemical composition was calculated using the ZAF correction method. In order to establish the operation conditions of the instrument, samples of Al_2O_3 and MoO_3 were used. The experimental results were compared with their theoretical compositions and a statistical study of the exactitude and precision of the instrument was determined (Ellison, et al., 1995). Subsequently, under these conditions samples containing $S-MoO_3$, $V_2O_5-TiO_2$ and SiO_2-WO_3 were analyzed and their average compositions were reported. Al_2O_3, MoO_3, S, V_2O_5, TiO_2, SiO_2 and WO_3 analytic grade were used to prepare the samples. Samples with 1, 5, 10 and 15 wt% of Mo were prepared for the $MoO_3-Al_2O_3$ system. Same S concentrations in the $S-MoO_3$ system were prepared. For the $V_2O_5-TiO_2$ system, the samples were prepared at 0.5, 1, 3, 5 wt% of V while the SiO_2-WO_3 system the tungsten concentration in the samples were 20, 40, 50 and 60 wt% of W. All samples were mechanically mixed in an agate mortar. $V_2O_5-TiO_2$ and SiO_2-WO_3 systems were mixed and annealed at 500 °C. In order to calculate the chemical composition of the elements, more intense characteristic energy lines were used. Five measurements in different region were performed in each sample. The concentration values reported of each component for each sample was the average value. A monolayer of sample was deposited and dispersed on carbon tape to have a flat surface.

3. Results and discussion

3.1 Review of the operation conditions of the instrument

The best operation conditions in the instrument to calculate the more accurate elemental chemical composition were established using Al_2O_3 and MoO_3 samples. These samples were selected because they are components of the hydrodesulfuration catalysts. Al_2O_3 and MoO_3 are very stable under environmental conditions of temperature, humidity and pressure. Their chemical composition remains constant with the time.

The effect of the Tc, AV and AT variables on the chemical composition was studied using MoO_3. Figure 1 shows the typical EDX spectra of the MoO_3 displaying their characteristic energy lines located at 0.523 keV for OKα, 2.015, 2.293, 2.394 keV, for MoLl, MoLα1 and MoLβ1 and 17.376, 17.481, 19.609 keV for MoKα2, MoKα1 and MoKβ1. All lines were displayed in five Gaussian peaks. The more intense peaks correspond to the OKα and MoLα1 lines. The software calculates the composition using the energy lines corresponding to the shell ionized, for instance the OK and MoL lines for MoO_3. The first calculus was made with the EDX spectrum obtained to a Tc of 35.0μs, 25kV AV, 100s of lecture, around 30% of DT, 11 mm of WD and 100X of magnification using the most intense peaks, OK and MoL lines. The results obtained were 32.30 wt% O and 67.70 wt% Mo, composition close to the theoretical composition (33.35 wt% O and 66.65 wt% Mo). This result differs of the results obtained with MoK line. The chemical composition obtained considering MoK line was 23.40 wt% O and 76.60 wt% Mo, composition very far of the theoretical composition. Here is important to note the importance of consider the more intense characteristic energy lines to obtain more accurate composition results in samples containing an element with two line series as K and L or M and L.
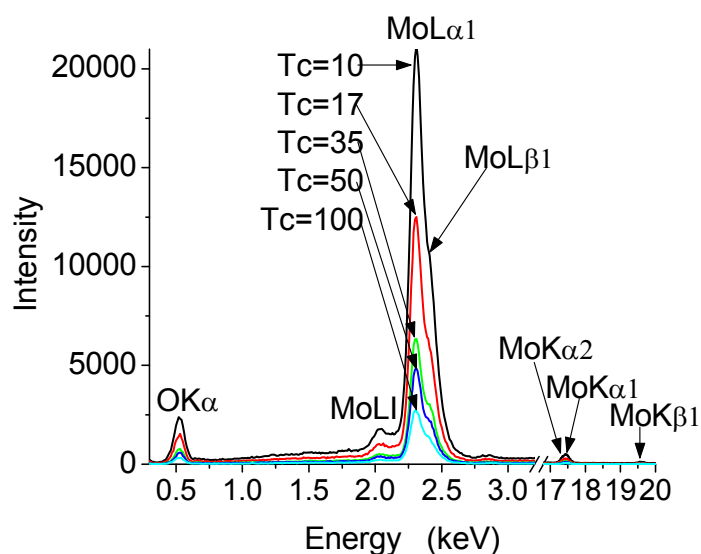

Fig. 1. EDX spectra showing the O and Mo experimental Gaussian peaks at different Tc. The spectra were obtained under operation conditions of DT around 30%, 25kV and 100s of acquisition time.

Knowing that with the MoL line the calculus of chemical composition gives a better approximation to the theoretical composition of MoO_3, the study of the effect of Tc in the chemical composition can be performed. Tc variable is the time allowed for the pulse processor to evaluate the magnitude time of pulse. For longer Tc, the ability of the system to assign an energy to the incoming pulse is better, but a few counts can be processed in a given analysis time. Therefore, longer Tc will give better spectrum resolution but the count rate will be lower. Shortest Tc will allow to process more counts per second but with a large error in the assignment of a specific energy to the pulse, and so the energy resolution will be poor. This can be observed in the Gaussian curves of MoO_3 EDX spectra displayed in Figure 1. A careful analysis of Figure 1 indicates that the resolution between the MoLα1 and MoLβ1 lines were better resolved at 100.0μs than at 10.0μs of Tc. In general, at shorter Tc larger intensity, wider broadening and minor resolution, while at higher Tc, minor intensity, minor

broadening and better resolution is obtained. Nevertheless, the peak intensity and its broadening are important in the calculus of the composition and the resolution is also important to discern the characteristic energy of the chemical elements and as it can be seen in the Gaussian curves of Figure 1, the intensity, broadening and resolution changes for each Tc measured. Its effect in the chemical composition is displayed in table 1. A relative error was calculated between the theoretical and experimental composition data to analyze the results. The relative error given in the last column is lesser than 2.5% and it does not show some tendency. This means that the Tc has little effect in the chemical composition. The larger and smaller error was obtained at Tc=50.0μs and Tc=100.0μs, respectively. Therefore, a Tc optimum must be choice without affect both, intensity and resolution, too much.   In the instrument used in this work the Tc value suggested by the provider was 35.0μs that combine resolution and intensity giving a relative error of 1.6%.

Tc(μs)	OK(Wt%)	MoL(Wt%)	Mo %Error
10	32.02	67.98	2.0
17	32.71	67.29	1.0
35	32.30	67.70	1.6
50	31.69	68.31	2.5
100	33.03	66.97	0.5

Table 1. Chemical composition of MoO_3 obtained with the OK and MoL lines at different time constant.

With a Tc=35.0μs and 100s of acquisition time, the effect of accelerating voltage on molybdenum oxide composition was studied. The DT was kept around of 30% manipulating the spot size. Figure 2 displays the EDX spectra of the OK and MoL characteristic energy lines. The Figure 2 shows a decreasing in the peak intensity with the increase of the accelerating voltage, see inset in Figure 2. However, the peak width fits with the others Gaussian peaks. This overlapping of curves was more evident for MoL line than OK line. The decreasing of the intensity produced by increase of the accelerating voltage without affect the broadening in the Gaussian curves suggests that the accelerating voltage has strong effect in the determination of the composition. This was revealed in the calculus of the composition, see table 2. At low accelerating voltage high error was obtained and it decreased with the increase of accelerating voltage obtaining the lowest error at 25 kV. Therefore, in order to obtain more accurate overall chemical composition is very important acquire experimental data at 25kV in the instrument used in this work for this sample.

Acc. Voltage (kV)	OK(Wt%)	MoL(Wt%)	Mo %Error
15	27.20	72.80	9.2
20	29.55	70.45	5.7
25	32.47	67.53	1.3
30	34.31	65.69	1.4

Table 2. Chemical composition of MoO_3 obtained with OK and MoL lines at different accelerating voltage.
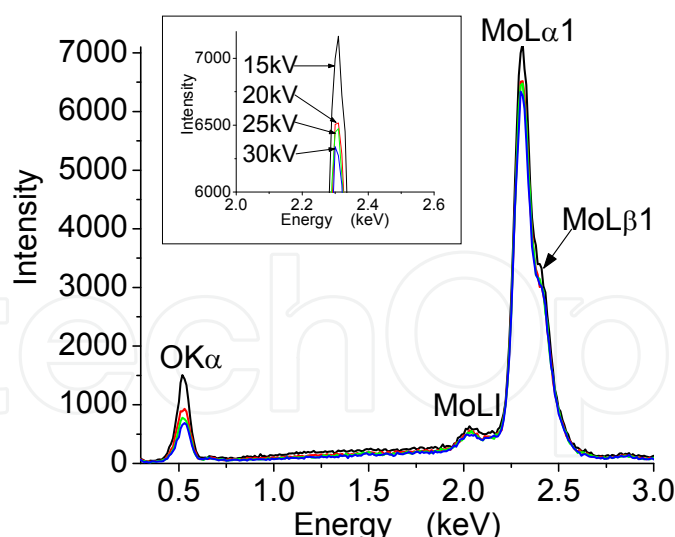
Fig. 2. EDX spectra showing the O and Mo experimental Gaussian peaks at different accelerating voltage. The spectra were obtained under operation conditions of Tc=35μs, DT around 30% and 100s of acquisition time.

The acquisition time is directly related with the intensity and it is expected to affect the calculus of the composition. Therefore, it is important to know how AT affects the MoO_3 composition and determine if there is an optimum acquisition time for more precise experimental results. Measurements carried out at Tc 35μs and 25kV and different acquisition time are displayed in the EDX spectra of Figure 3. The Gaussian peaks of the OK and MoL lines show an increase in the intensity and broadening with an increase on the acquisition time. This behavior suggests that the acquisition time has little effect in the chemical composition as it was revealed in the calculus displayed in table 3. A relative error of 1.7% was obtained at 100 and 200s of lecture while at 300 and 400s the error obtained was 1.4%. Therefore, the time acquisition only minimizes the integration error of the experimental results, and it does not affect the chemical composition. An acquisition time of 100s is adequate for performance the chemical analysis.
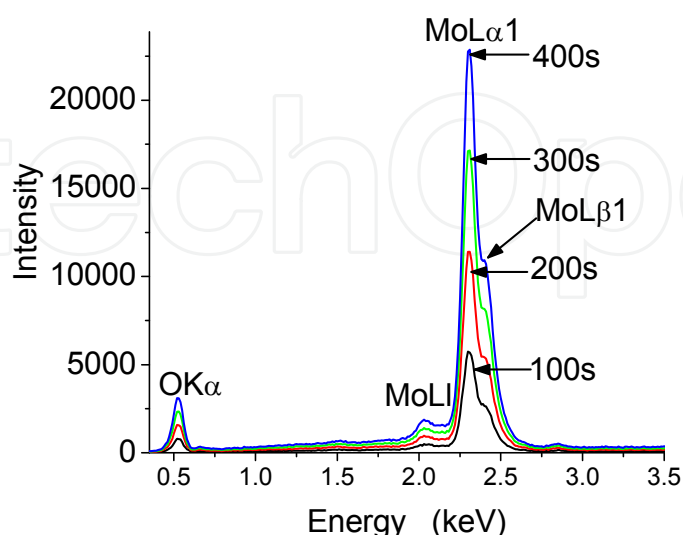

Fig. 3. EDX spectra showing the O and Mo experimental Gaussian peaks at different acquisition time. The spectra were obtained under operation conditions of Tc=35μs, DT around 30% and 25kV.

Acquisition Time(s)	OK(Wt%)	MoL(Wt%)	Mo %Error
100	34.48	65.52	1.7
200	34.50	65.50	1.7
300	34.25	65.75	1.4
400	34.30	65.70	1.4

Table 3. Chemical composition of MoO_3 obtained with OK and MoL lines at different acquisition time.

Knowing the values of the variables as Tc, accelerating voltage and acquisition time, the instrumental error was estimated performing measurements in a same region for five times. The measurements were performed at 35.0μs of Tc, 25kV of accelerating voltage 100s of acquisition time, around of 30% of DT, 100X of magnification and 11mm of WD. The results obtained are displayed in EDX spectra of Figure 4. As expected, the Gaussian peaks of the OK and MoL energy lines overlap with each measurement in the EDX spectra; however, the variations in the intensity of the peaks without affecting their broadening could affect the results of the chemical composition as was observed previously in the voltage study. These variations are related with the ability of the instrument to reproduce a measurement. The composition results and the relative errors calculated for every measurement is illustrated in table 4. As can be seen, the composition in every measurement is different indicating the instrumental error in the determination of the chemical composition. The variations are small without show any tendency. Under the measurement conditions used, the average error for the O was 1.9% while for the Mo it was 0.9%. From these results, it is possible to calculate the accuracy and precision of the instrument. Therefore, the instrument has an accuracy around 0.6wt% and a precision around 0.2wt%.
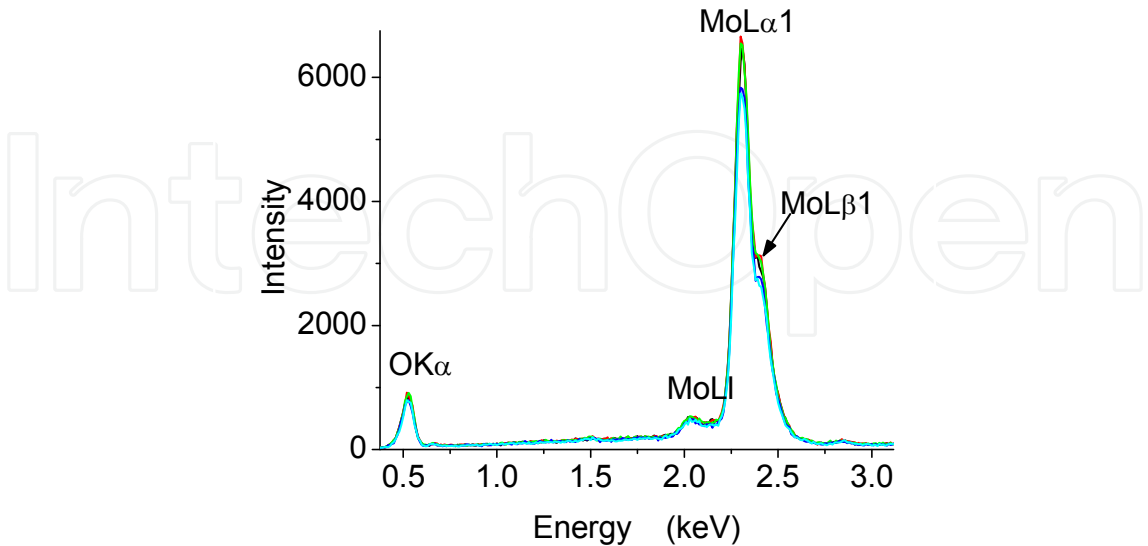

Fig. 4. EDX spectra showing the O and Mo experimental Gaussian peaks obtained in a same region under operation conditions of Tc=35μs, 25kV, DT around 30% and 100s of acquisition time.

Measurement	OK(Wt%)	O %Error	MoL(Wt%)	Mo %Error
1	33.44	0.3	66.56	0.1
2	34.04	2.1	65.96	1.0
3	34.16	2.4	65.84	1.2
4	33.75	1.2	66.25	0.6
5	34.48	3.4	65.52	1.7
Average	33.97	1.9	66.03	0.9

Table 4. Chemical composition of MoO_3 obtained with OK and MoL lines in the same analysis region.

Once the precision and exactitude of the instrument are known, the homogeneity of the O, Al and Mo composition in the Al_2O_3 and MoO_3 samples was evaluated. As the samples analyzed were analytical grade is expected a homogenous chemical composition and then the measurement error will be equal or minor to the instrumental error. To carry out the study, ten measurements in different regions of the Al_2O_3 sample deposited on the carbon tape were obtained using the same operation conditions of the instrument to determine the instrumental error. The results obtained are displayed in table 5. Characteristic energy corresponding to OK and AlK lines located at 0.523 and 1.486 keV were used to calculate the composition. Chemical composition expected is 47.07 wt% O and 52.93 wt% Al. This theoretical chemical composition was used in the statistical analysis. The average experimental composition obtained was around 46.46 wt% O and 53.54 wt% Al. The average calculated error was around of 1.3% for O and 1.2% for Al. The precision calculated for this sample was around of 0.2 wt% and the exactitude was around 0.6 wt%. The results are similar to the obtained in the study of the instrumental error. This similitude is indicating the high homogeneous distribution of the O and Al atoms in the alumina sample. Then, the measurement error is attributed to the instrument.

Measurement	OK(Wt%)	O %Error	AlK(Wt%)	Al %Error
1	46.85	0.5	53.15	0.4
2	46.42	1.4	53.58	1.2
3	46.70	0.8	53.30	0.7
4	46.07	2.1	53.93	1.9
5	46.47	1.3	53.53	1.1
6	46.92	0.3	53.08	0.3
7	46.80	0.6	53.20	0.5
8	46.74	0.7	53.26	0.6
9	46.49	1.2	53.51	1.1
10	45.14	4.1	54.86	3.6
Average	46.46	1.3	53.54	1.2

Table 5. Chemical composition of Al_2O_3 obtained with OK and AlK lines in different regions of the sample.

Experimental results corresponding to the molybdenum oxide is displayed in table 6. OK and MoL characteristic lines were used to calculate the chemical composition. In this sample, the average experimental composition obtained was 32.86 wt% O and 67.14 wt% Mo. The average measurement error calculated was 1.3% for O and 1.2% for Mo with an accuracy and precision of 0.5wt% and 0.3wt%, respectively. The exactitude value is into range calculated for the instrument but not for the precision. Precision is the degree of dispersion of the data, and then the result is indicating a high dispersion of the values of oxygen and molybdenum composition in the sample compared with the dispersion produced by the instrument. This dispersion could be related with the homogeneity grade in the chemical composition of the sample.

Measurement	OK(Wt%)	O %Error	MoL(Wt%)	Mo %Error
1	32.83	1.6	67.17	0.8
2	32.17	3.5	67.83	1.8
3	33.19	0.5	66.81	0.2
4	32.17	3.5	67.83	1.8
5	34.48	-3.4	65.52	-1.7
6	33.44	-0.3	66.56	-0.1
7	32.47	2.6	67.53	1.3
8	33.53	-0.5	66.47	-0.3
9	32.31	3.1	67.69	1.6
10	32.02	4.0	67.98	2.0
Average	32.86	1.5	67.14	0.7

Table 6. Chemical composition of MoO_3 obtained with OK and MoL lines in different regions of the sample.

3.2 MoO_3-Al_2O_3 system

With the operation conditions established on the instrument and knowing the exactitude and precision grade, a study on the determination of molybdenum in alumina was carried out. The purpose was to evaluate the response capability of the instrument to quantify molybdenum at different concentration in the alumina matrix. Theoretically, the instrument can detect concentrations around of 0.1wt% under special operation conditions. In this study, the samples analyzed were prepared with nominal molybdenum concentration of 1, 5, 10 and 15wt%. The results obtained are displayed in the EDX spectra of Figure 5. The more intense Gaussian peaks corresponding to the OK, AlK and MoL characteristic energy lines are observed. Figure 5 shows the EDX spectra of MoO_3/Al_2O_3 system with low and high Mo concentration. As expected, at low Mo concentration the MoL Gaussian peak is very small, while at high Mo concentration the MoL Gaussian peak is more intense indicating the qualitative increase of Mo. Additionally, in the Gaussian peaks can be observed the calculated curve, black line, overlapping the experimental curve, red line. Observing the difference between both curves, a very well fit can be determined. Latter indicates that all necessary considerations were made for a good interpretation of the experimental results. This analysis is very important when in the samples are present elements with very close characteristic energy lines that cannot be resolved by the

instrument and/or when the concentration of one of the components is very low that cannot be detected its corresponding characteristic energy lines. Generally, the next energy line occurs at high energy value; for molybdenum the next energy line is the MoK and it is not detected at low concentration. Then, a careful analysis of calculated and experimental curves helps to resolve the presence of elements with characteristic energy lines very close and consequently their concentration can be calculated. The following systems analyzed in this work correspond to some examples to resolve the problematic presented when elements with similar energy lines are containing in a specimen. As can seen in the Figure 5, both EDX spectra the experimental and calculated curves follow the same trajectory indicating that chemical elements identified in the sample were correct. The average chemical composition calculated for each sample is displayed in table 7. Each molybdenum value obtained was into measurement error. Therefore, the results obtained operating the instrument under the conditions previously mentioned were enough reliable.
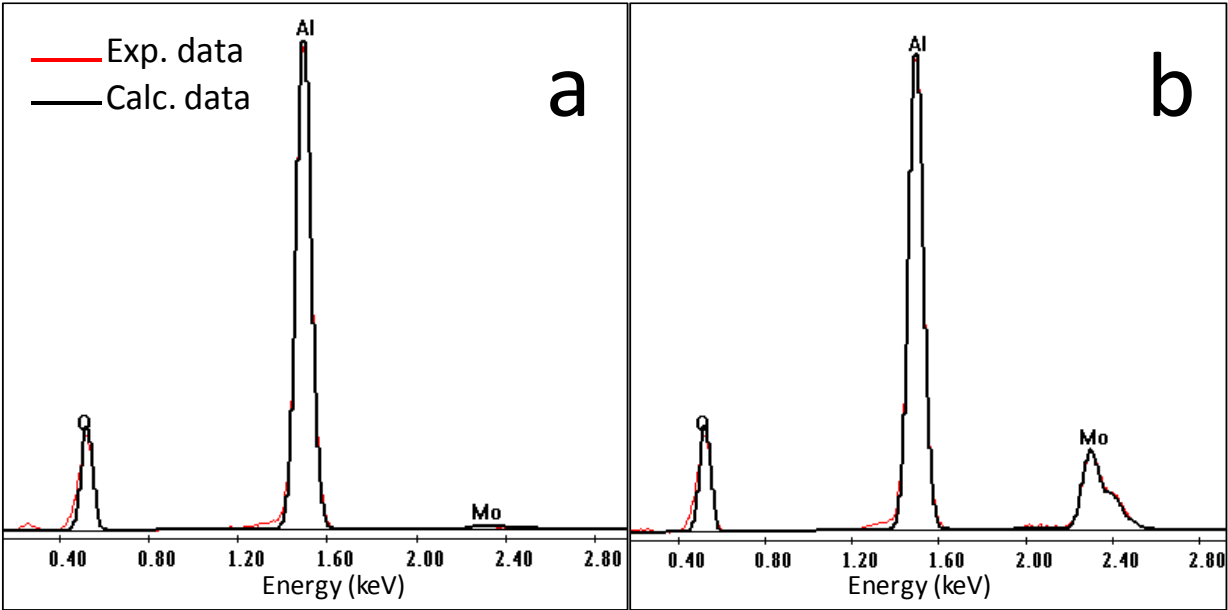
Fig. 5. EDX spectra showing the peak intensities corresponding to OK, AlK and MoL lines a)l.0 Wt% Mo and b)15Wt% Mo

Nominal Mo (Wt%)	O (Wt%)	Al (Wt%)	Mo (Wt%)
1	45.82	52.85	1.33
5	46.44	48.36	5.2
10	45.58	44.64	9.78
15	46.30	42.80	15.23

Table 7. Average chemical composition of the O, Al and Mo obtained of Al_2O_3 and MoO_3 samples at different molybdenum compositions.

3.3 S-MO₃ system

According with the previous results, measurements into the reliability range marked by the instrumental error can be obtained. Now, the capabilities of the instrument to resolve the

chemical composition of two elements that have characteristic energy values very close were analyzed. The first example was the determination of S in S-MoO$_3$ samples. Their more intense characteristic energy lines are very close and when both components are present in the sample only one experimental Gaussian peak is generated overlapping the presence of both elements. The case was studied using an S-MoO$_3$ system where sulfur concentration was varied from 1 to 15 wt%. Experimentally, one Gaussian peak was detected in the EDX spectrum. Figure 6 shows experimental Gaussian peak around of SK and MoL lines in the sample with the lower sulfur concentration. This experimental curve can be explained if we analyzed the values of the characteristic energies of both elements. The characteristic energies of the sulfur are SKα and SKβ with values of 2.307 and 2.464 keV while for molybdenum are MoLI, MoLα and MoLβ with values of 2.015, 2.293 and 2.394 keV, respectively. The energy difference between more intense lines, SKα and MoLα, is 0.014 keV and the energy resolution of the instrument is 0.129 keV, which is larger than the separation between both energies. Therefore, only one experimental Gaussian peak is generated, see Figure 6. A careful analysis the Gaussian peaks evidence the presence of Mo by the presence of MoLβ line that it is separated 0.101 keV from MoLα line and 0.087 keV from SKα line. However, the SKα line is contained in it. To evidence the presence of sulfur component the overlapping of the calculated Gaussian peak with the experimental was made considering first individual elements and after both of them. The results obtained are displayed in Figure 6 for the sample with 1wt% S. Figure 6a show the calculated Gaussian curve considering only SK line, the fit with the experimental Gaussian curve was not good, see Figure 6a. Considering only the MoL line the calculated and experimental Gaussian curves are very close, Figure 6b, however, in the maximum of the calculated peak does not match with the maximum of the experimental one. The calculated curve is shift to the left of the experimental curve. In Figure 6c, both SK and MoL lines were considered in the calculus and the result obtained is lightly better than that obtained with individual MoL line in Figure 6b. As both results of Figure 6b and c almost are likeness, the presence of S in the sample can be doubtful. Then, the deconvolution and composition results must be reviewed. An integration error is given by the Phoenix software after chemical composition calculation. This error must be below 10% and for the analysis of sulfur in this sample was around 2.5% indicating good fit and confirming the presence of sulfur in the sample.
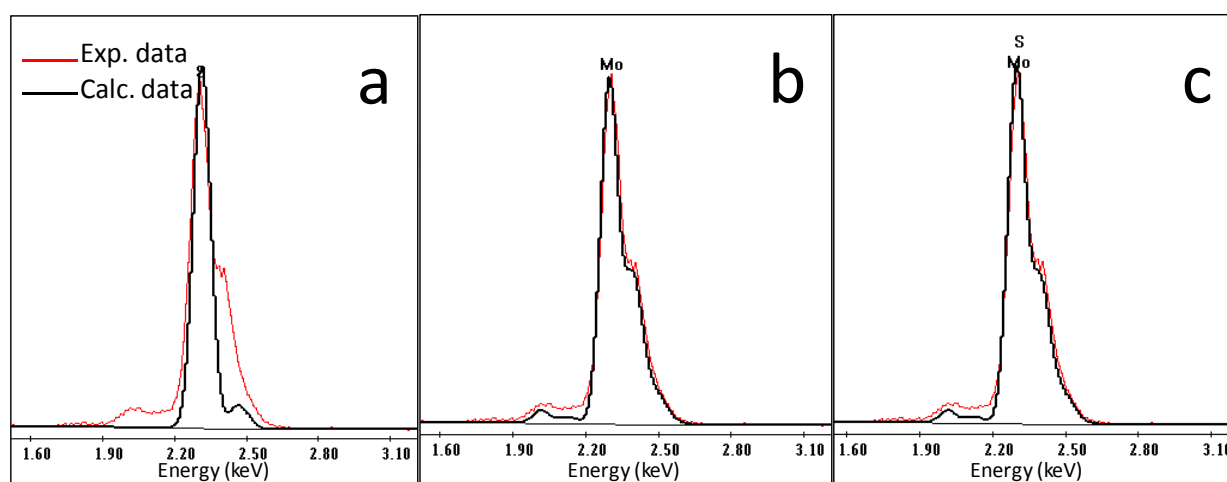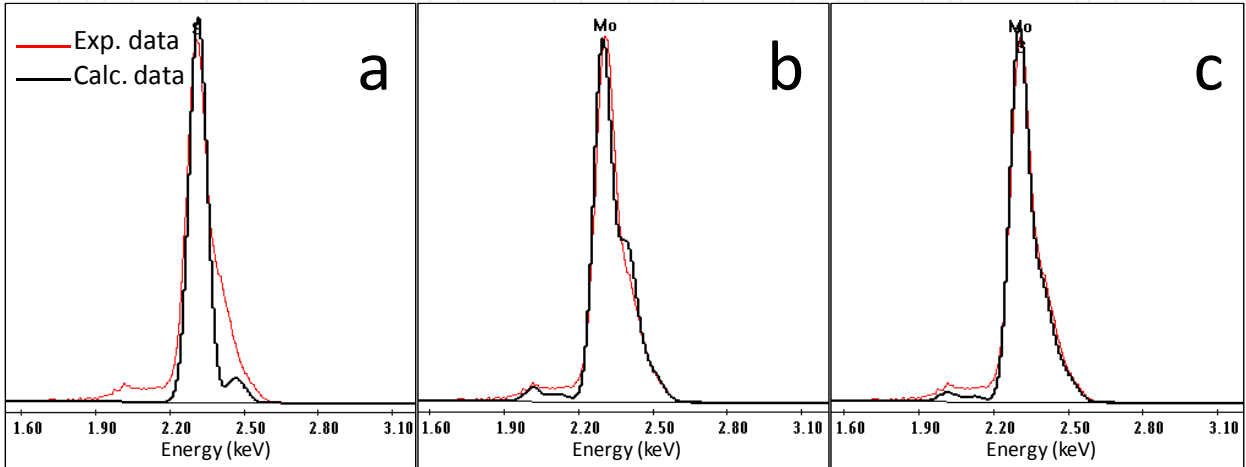

Fig. 6. EDX spectra of the sample with 1 wt% S showing the experimental and calculated Gaussian curves around of the SK and MoL lines. Calculated Gaussian curve considering a) SK line b)MoL line and c) SK and MoL lines.

When the sulfur content is increased, the shape of the experimental curve is modified, see Figure 7. The shoulder generated by the MoLβ line was disappearing with the increase of the S concentration. In this case is easy to follow the presence of sulfur in the experimental curve. Calculated curves with individual SK or MoL line do not match the experimental Gaussian curve, Figure 7a and 7b. However, when both SK and MoL lines are considered, the calculated Gaussian curve match very well the experimental curve indicating the presence of both elements with high reliability grade, see Figure 7c. The integration error of the SK was below of 1% which is good.

Fig. 7. EDX spectra of the sample with 15 wt% S showing the experimental and calculated Gaussian curves around of the SK and MoL lines. Calculated Gaussian curve considering a) SK line b)MoL line and c) SK and MoL lines

After the accurate identification of the chemical components in the EDX spectrum, the chemical composition of each sample was obtained. The average chemical composition of every component is displayed in table 8. The sulfur concentration values displayed in the last column are near to the nominal composition. The variations observed can be due to manipulation error during the preparation of the samples. The results indicate that not homogeneous samples were prepared by physical mixing. Another preparation route must be proposed for standard samples preparation. Nevertheless, for the purpose of measure the capability of the instrument to calculate the chemical composition of two elements with close characteristic energy lines that generate just one experimental Gaussian peak, the experimental values obtained were good.

Nominal S (Wt%)	O (Wt%)	Mo (Wt%)	S (Wt%)
1	31.87	66.47	1.56
5	30.81	64.76	4.33
10	28.47	60.91	10.62
15	27.95	58.11	13.89

Table 8. Average chemical composition of the O, Mo and S obtained of S and MoO_3 samples at different sulphur composition.

3.4 WO₃-SiO₂ system

The WO$_3$-SiO$_2$ system presents the same problematic with their corresponding more intense SiKα and WMα1 lines, they overlap giving rise only a Gaussian peak in the EDX spectrum. Therefore, it is not easy to evidence Si at low concentrations when the W is present at high concentration and vice-versa, because all energies of the SiK and WM are very close and at low tungsten concentration, the WLα line is not detected. Therefore, a carefully analysis of the experimental Gaussian peak generated by the presence of both elements must be carried out. In order to know the capability of the instrument to calculate the Si and W compositions using only one experimental curve containing the characteristic energy lines of both elements, SiO$_2$ and WO$_3$ mixed samples with concentration of 20, 40, 50 and 60 wt% of W were prepared. Just one experimental Gaussian peak was obtained for SiK and WM lines for the sample with 20 wt% W, Figure 8, making very difficult to evidence the presence of both Si and W components. The values of the characteristic energies of the SiK are 1.740 keV for SiKα and 1.829 keV for SiKβ. For WM are 1.776 keV for WMα1, 1.835 keV for WMβ, 2.035 for WMγ and 1.379 keV for WMz2. And the energy difference between SiKα and WMα1 lines is 0.036 keV which remain also below limit of energy resolution of the instrument (0.129 keV). For the analysis, first the presence just SiK line was considered in the calculus and it do not match very well with the experimental curve, Figure 8a. The calculated curve is shifted lightly to the left of the experimental Gaussian peak. In figure 8b shows the results obtained considering only WM line. The calculated Gaussian curve deviates strongly from the experimental one. In this case, the calculated curve is shifted to the right of the experimental curve and its calculated peak intensity stayed below the intensity of the experimental peak. Considering the presence of both elements, the calculated Gaussian peak with SiK and WL lines match very well the experimental Gaussian peak, Figure 8c. The WM and SiK integration error obtained for this sample was below 1%, and then the presence of both elements was confirmed.
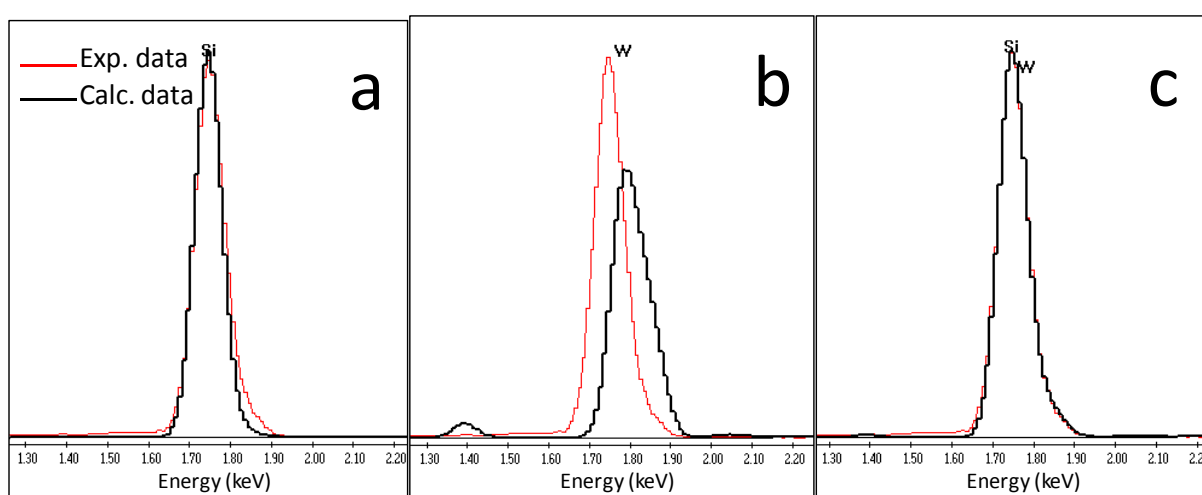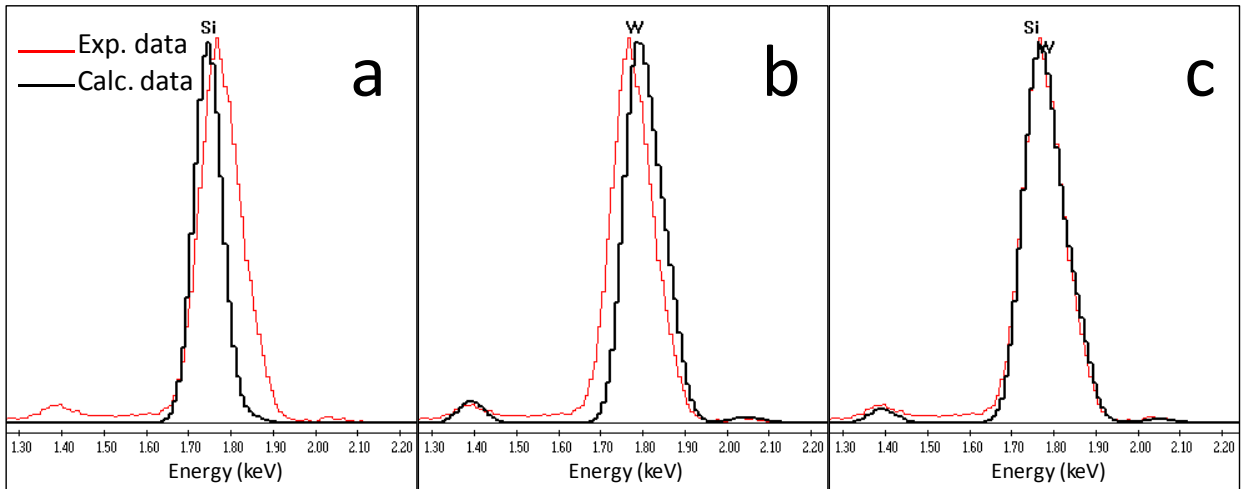

Fig. 8. EDX spectra of the sample with 20 wt% W showing the experimental and calculated Gaussian curves around of the SiK and WM lines. Calculated Gaussian curve considering a) SiK line b) WM line and c) SiK and WM lines

At higher tungsten concentrations (60 wt% W), the calculated Gaussian curve obtained considering only the presence of SiK line do not match with the experimental curve as is illustrated in Figure 9a. The calculated curve is shifted to the left of the experimental curve, whereas when just WM line is considered, the calculated Gaussian curve is shifted to the right of the experimental curve Figure 9b. Figure 9c shows the results obtained considering the SiK and WM lines in the calculus, the experimental Gaussian curve was fitted very well with the presence of both characteristic energy lines in the calculus. The integration error for SiK and WM remain below 1%. The error of integration is useful when the concentration of a component is low. When the concentration of the component is high, the integration error will be always less than 1%. Then, for these samples with the analysis of the Gaussian curve is enough.

Fig. 9. EDX spectra of the sample with 60 wt% W showing the experimental and calculated Gaussian curves around of the SiK and WM lines. Calculated Gaussian curve considering a) SiK line b) WM line and c) SiK and WM lines

After determination of the presence of SiK and WL in the experimental Gaussian curve, the chemical composition on samples with different tungsten concentration was calculated. The obtained results are displayed in the table 9. The W compositions are close to the nominal composition. The deviation between the nominal and experimental results was around 1 to 1.7 wt % which can be attributed again to the manipulation process during the sample preparation. However, the results obtained are reliable and the fit of the experimental curve considering two elements has the ability to discern the composition of each element.

Nominal W (Wt%)	O (Wt%)	Si(Wt%)	W (Wt%)
20	40.78	40.74	18.48
40	33.47	27.23	39.30
50	28.67	19.64	51.69
60	24.63	14.40	60.97

Table 9. Average chemical composition of the O, Si and W obtained of SiO_2 and WO_3 samples at different tungsten composition.

3.5 V_2O_5-TiO_2 system

In this section will be analyzed the ability of the instrument to calculate the chemical composition in samples where the more intense characteristic energy line of one element is overlapped to one characteristic energy line of low intensity of the other component, specifically Kα line with Kβ line. This case is generally present in transition metals, and the V_2O_5-TiO_2 system was selected for this study. This problem occurs when one component is present at low concentrations, usually less than 5 wt% as in the case of vanadium. At V concentration below 5 wt% VKα line is too low and overlapped with TiKβ line of Ti. For this propose mechanical mixture of V_2O_5 and TiO_2 at vanadium concentration of 0.5, 1, 3 and 5 wt% were prepared. Figure 10 shows experimental Gaussian curve obtained corresponding to the TiKα and TiKβ lines of the sample with 0.5 wt% of V. Only one experimental Gaussian peak around of the VKα and TiKβ lines was observed, then, a careful analysis of the experimental curve to evidence the presence of V is necessary. The characteristic energies of Ti are located at 4.508 keV for TiKα and at 4.931 keV for TiKβ1 while for the V they are at 4.948 keV for VKα and at 5.426 keV for VKβ1. The more intense energies for Ti and V are TiKα and VKα which are resolved by the instrument at high concentrations; however at low vanadium concentration the intensity of VKα line is overlapped with the TiKβ1 line. Between these lines there is a difference of 0.017 keV which is below limit of energy resolution of the instrument, so only an experimental Gaussian curve is showed in Figure 10. The calculated Gaussian peak considering only the presence of TiK is displayed on the experimental Gaussian curve of Figure 10a. The calculated curve does not match with the experimental curve at VKα and TiKβ1 energy values. The calculated Gaussian curve is shifted to the left from the experimental Gaussian curve. For comparison, an EDX spectrum of a pure titanium oxide sample was obtained in which the calculated Gaussian curve for TiK line matched with the experimental one, see Figure 11. Therefore, the deviation observed in Figure 10a indicates qualitatively the presence of V in the sample. Considering both VK and TiK lines, the calculated Gaussian curve matched very well the experimental Gaussian curve. In this case, it is important to use the integration error to obtain better evidence of V presence in the sample. The integration error obtained with the VK line was around of 7% remaining lesser than 10%, confirming the presence of V in the sample.

At 5 wt% V concentration, a small Gaussian peak located at 5.426 keV corresponding to the VKβ1 line was detected in Figure 12, and then the presence of vanadium is easily identified. However, if only TiK line is considered the calculated curve do not match with the experimental curve at TiKβ line, Figure 12a. The position and intensity of calculated curve is different and is shifted to the left. This is less intense than the experimental curve. Therefore, the experimental Gaussian peak indicates the presence of VKα characteristic energy line. The calculated Gaussian curve considering the TiK and VK lines is showed in Figure 12b. This result matches very well the experimental Gaussian curve. Additionally, the small experimental Gaussian curve corresponding to the VKβ1 line is also fitted.

After analysis of the vanadium presence in the Gaussian peaks in the EDX spectrum, the chemical composition of samples with different V loading was obtained. The results are displayed in the table 10. As it can be observed, the vanadium concentrations are close to the nominal composition, confirming the capability of the instrument to give the composition of the chemical elements when their corresponding energy lines are close and their presence cannot be resolved by the instrument generating only one experimental Gaussian peak for both elements.
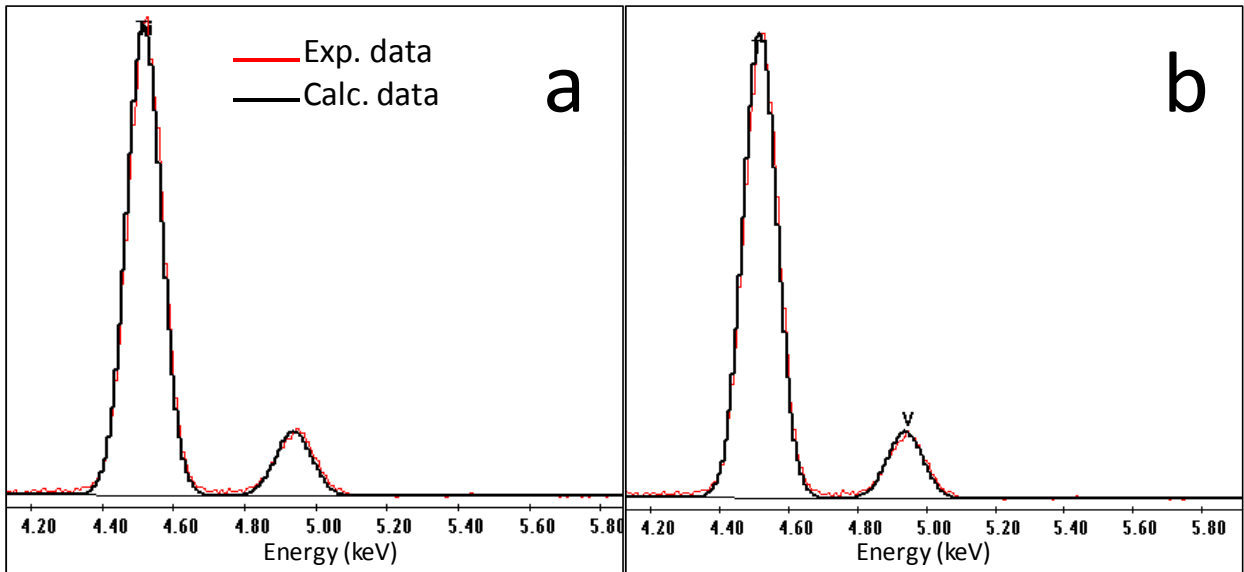
Fig. 10. EDX spectra of the sample with 0.5 wt% V showing the experimental and calculated Gaussian curves around of the TiK and VK lines. Calculated Gaussian curve considering a) TiK line and b) VK and TiK lines
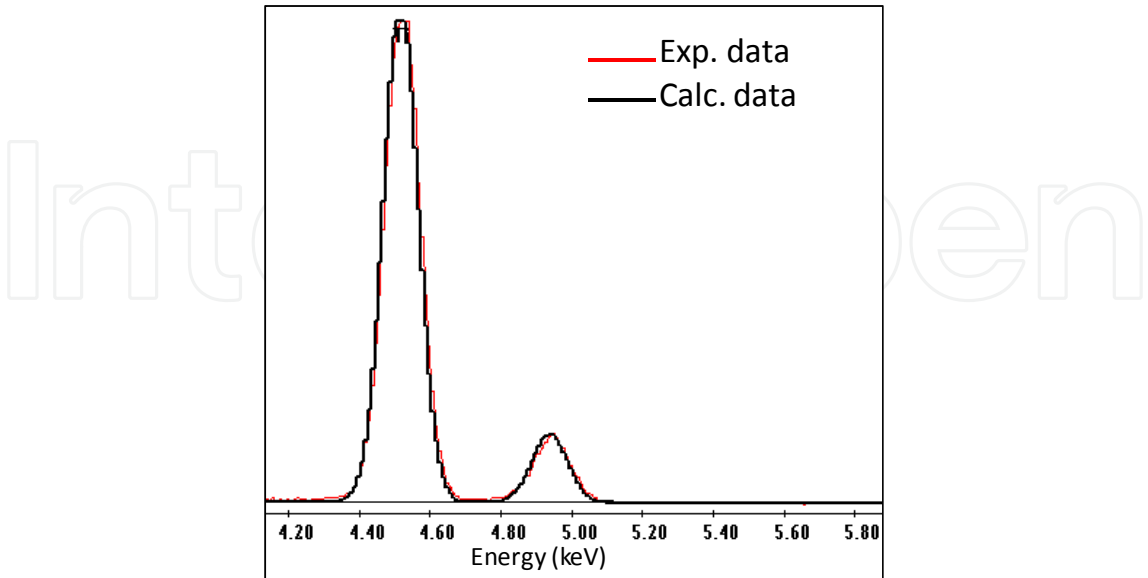

Fig. 11. EDX spectrum of a titanium oxide sample showing the calculated Gaussian curves with the TiK line. The calculated Gaussian peaks fit very well the experimental curves.
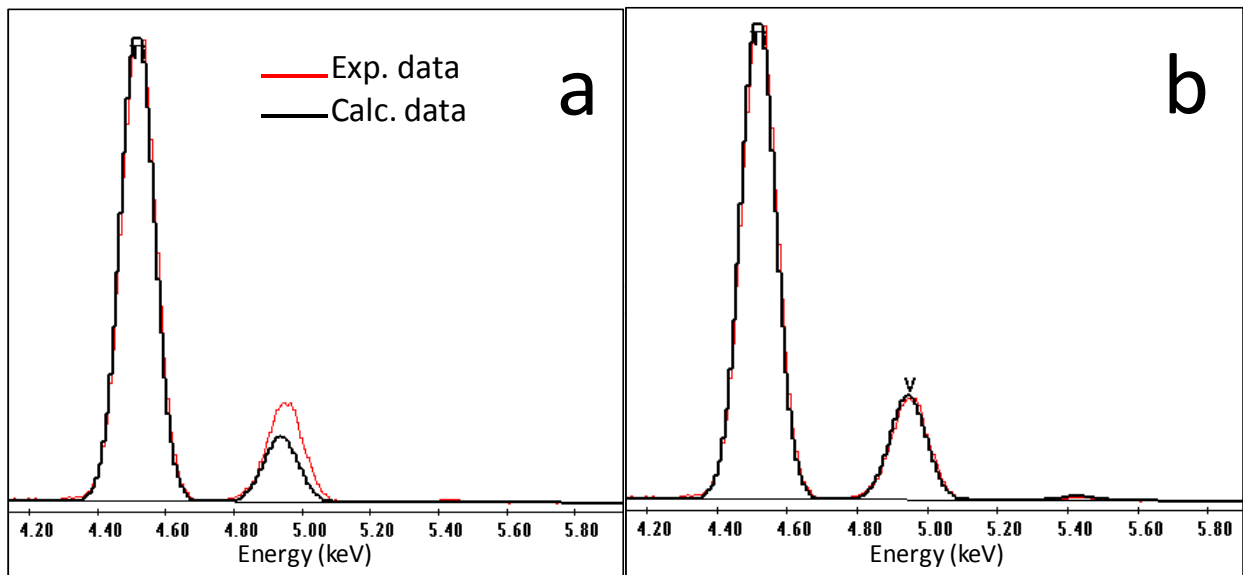
Fig. 12. EDX spectra of the sample with 5 wt% V showing the experimental and calculated Gaussian curves around of the TiK and VK lines. Calculated Gaussian curve considering a) TiK line and c) VK and TiK lines

Nominal V (Wt%)	O (Wt%)	Ti (Wt%)	V (Wt%)
0.5	44.97	54.36	0.67
1	42.47	56.75	0.78
3	43.40	54.20	2.39
5	41.69	53.79	4.52

Table 10. Average chemical composition of the O, Ti and V obtained from samples of V_2O_5 and TiO_2 at different vanadium composition.

4. Conclusion

The optimization of the operation conditions of the instrument to obtain more reliable elemental chemical composition for alumina and molybdenum oxide was reviewed. For the environmental scanning electron microscope PHILIPS XL30 the better operation conditions were a constant time of 35μs, 25kV of accelerating voltage and 100s of acquisition time keeping constant the dead time, the magnification, and the work distance. Under these operation conditions the exactitude and precision of the instrument to calculate the O, Al and Mo compositions for the alumina and molybdenum oxide was 0.6wt% and 0.2wt%, respectively. The more intense characteristic energy lines must be used to calculate the composition. The instrument is able to resolve very well the chemical composition in samples having elements with their more intense characteristic energy lines overlapped and they cannot be resolved by the limit of energy resolution of the instrument. Additionally, the preparation of the sample to be analyzed by SEM plays an important role for the determination of the chemical composition, then; a study of powder sample preparation is suggested. The results reported in this work correspond only to the samples analyzed with the instrument used.

5. Acknowledgment

6. References

Angeles, C.; Rosas, G. & Perez, R. (2000). Preparation of Al_3Ti and $L1_2$ Al_3Ti-Base Alloys Microalloyed with Fe By a Melting/Casting Rapid-Solidification Technique. *Materials and Manufacturing Processes*, Vol.15, No.2, (published 2000), pp.207-209, ISSN 1042-6914

Cortes-Jacome, M.A.; Toledo, J.A., Angeles-Chavez, C., Aguilar, M. & Wang, J.A. (2005). Influence of Synthesis Methods on Tungsten Dispersion, Structural Deformation, and Surface Acidity in Binary WO_3-ZrO_2, *Journal Physical Chemistry B*, Vol.109, No.48, (December 2005), pp. 22730-22739, ISSN 1520-6106

Goldstein, J.I. & Newbury, D.E. (2003). *Scanning Electron Microscopy and X-Ray Microanalysis*, Kluwer Academic, ISBN 0-306-47292-9, New York, USA

Williams, D.B . & Barry-Carter, C. (1996). *Transmission Electron Microscopy*, Plenum Press, ISBN 0-306-45247-2, New York, USA

Jenkins, K. & De Drier, J.L. (1967). *Practical X-Ray Spectrometry*, Springer-Verlag, BCIN No. 61267

Herglof, H. & Birk, L.S. (1978). *X-ray Spectrometry*, Dekker, ISBN-8247-6625-3, New York, USA

Deutsch, M.; Gang, O., Hamalainen, K. & Kao, C.C. (1996). Onset and Near Threshold Evolution of the Cu Kα X-Ray Satellites, *Physical Review Letters*, Vol.76, No.14, (April 1996), pp. 2424-2427, ISSN 0031-9007

Liebhafsky, H. A. (1976). *X-ray, Electrons, and Analytical Chemistry: Spectrochemical Analysis with X-rays*, Wiley- Interscience, ISBN 0471534285, New York, USA

Kenik, E.A. (2011). Evaluating the performance of a commercial Silicon Drift Detector for X-Ray Microanalysis, *Microscopy Today*, Vol.19, No.3, (May 2011), pp. 40-46, ISSN 1551-9295

Schlossmacher, P.; Kenov, D.O., Fritag, B. & Von Harrach, H.S. (2010). Enhanced Detection Sensitivity with a New Windowless XEDS System for AEM Based on Silicon Drift Detector Technology, *Microscopy today*, Vol.18, No.4, (July 2010), pp.14-20, ISSN 1551-9295

Newbury, D.E.; Joy, D.C., Echlin, P., Fiori, C.E. & Goldstein, J.I. (1986). *Advanced Scanning Electron Microscopy and X-Ray Microanalysis*, Plenum Press, ISBN 0-0306-42140-2, New York, USA

Chung, F.H.; Lentz, A.J. & Scott, R.W. (1974). Thin Film for Quantitative X-ray Emission Analysis, *X-ray Spectrometry*, Vol.3, No.4, (April 2005), pp. 172-175, ISSN 1097-4539

Ellison, S.L.R.; Roselein, M. & William, A. (1995). *Quantifying Uncertainty in Analytical Measurement*. EURACHEM/CITAC, ISBN 0-948926-08-2, London.
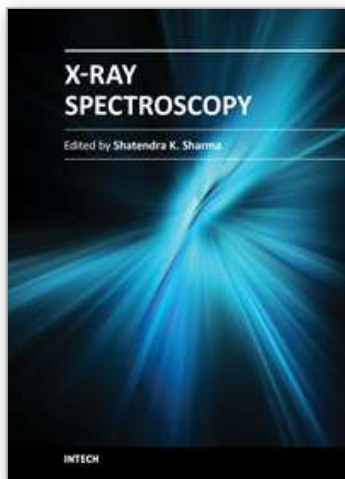
X-Ray Spectroscopy

Edited by Dr. Shatendra K Sharma

The x-ray is the only invention that became a regular diagnostic tool in hospitals within a week of its first observation by Roentgen in 1895. Even today, x-rays are a great characterization tool at the hands of scientists working in almost every field, such as medicine, physics, material science, space science, chemistry, archeology, and metallurgy. With vast existing applications of x-rays, it is even more surprising that every day people are finding new applications of x-rays or refining the existing techniques. This book consists of selected chapters on the recent applications of x-ray spectroscopy that are of great interest to the scientists and engineers working in the fields of material science, physics, chemistry, astrophysics, astrochemistry, instrumentation, and techniques of x-ray based characterization. The chapters have been grouped into two major sections based upon the techniques and applications. The book covers some basic principles of satellite x-rays as characterization tools for chemical properties and the physics of detectors and x-ray spectrometer. The techniques like EDXRF, WDXRF, EPMA, satellites, micro-beam analysis, particle induced XRF, and matrix effects are discussed. The characterization of thin films and ceramic materials using x-rays is also covered.

How to reference

In order to correctly reference this scholarly work, feel free to copy and paste the following:

Carlos Angeles-Chavez, Jose Antonio Toledo-Antonio and Maria Antonia Cortes-Jacome (2012). Chemical Quantification of Mo-S, W-Si and Ti-V by Energy Dispersive X-Ray Spectroscopy, X-Ray Spectroscopy, Dr. Shatendra K Sharma (Ed.), ISBN: 978-953-307-967-7, InTech, Available from: http://www.intechopen.com/books/x-ray-spectroscopy/chemical-quantification-of-mo-s-w-si-and-ti-v-by-energy-dispersive-x-ray-spectroscopy

INTECH
open science | open minds